Catalysis Letters (2019) 149:1224–1236
https://doi.org/10.1007/s10562-019-02703-z

Bioinspired Palladium Nanoparticles Supported on Soil-Derived Humic Acid Coated Iron-Oxide Nanoparticles as Catalyst for C–C Cross-Coupling and Reduction Reactions

Anurag N. Chinchole[1] · Abhishek V. Dubey[1] · A. Vijay Kumar[1]

Received: 29 October 2018 / Accepted: 4 February 2019 / Published online: 21 February 2019

Abstract

Pd nanoparticles supported on humic acid-coated nanoferrites as magnetically-recoverable catalyst was expediently prepared from inexpensive precursors and characterized by techniques such as SEM, TEM, XPS, FT-IR, XRD, ICP-AES, EDX. The as made catalyst displayed an admirable catalytic activity towards the Suzuki–Miyaura cross-coupling reaction of aryl halides (or) aryl diazonium salts with aryl boronic acid in non-toxic solvent EtOH/water under mild conditions. The same catalyst showed high efficiency for the Heck reaction of aryl halides with styrene was carried out with high efficiency offering good yields under ligand-free conditions. Additionally, the reduction of olefins using molecular hydrogen was also achieved using the same catalyst under ambient and base-free conditions affording the products in good to excellent yields. The magnetic activity of nano-Fe_3O_4 allowed the effortless recovery of the catalyst and demonstrated subsequent recyclability up to 5 cycles without a significant loss in the activity.

Anurag N. Chinchole and Abhishek V. Dubey have contributed equally.

Electronic supplementary material The online version of this article (https://doi.org/10.1007/s10562-019-02703-z) contains supplementary material, which is available to authorized users.

✉ A. Vijay Kumar
vijayakki@gmail.com

[1] Department of Chemistry, Institute of Chemical Technology, Nathalal Parekh Marg, Matunga, Mumbai, Maharashtra 400019, India

Graphical Abstract

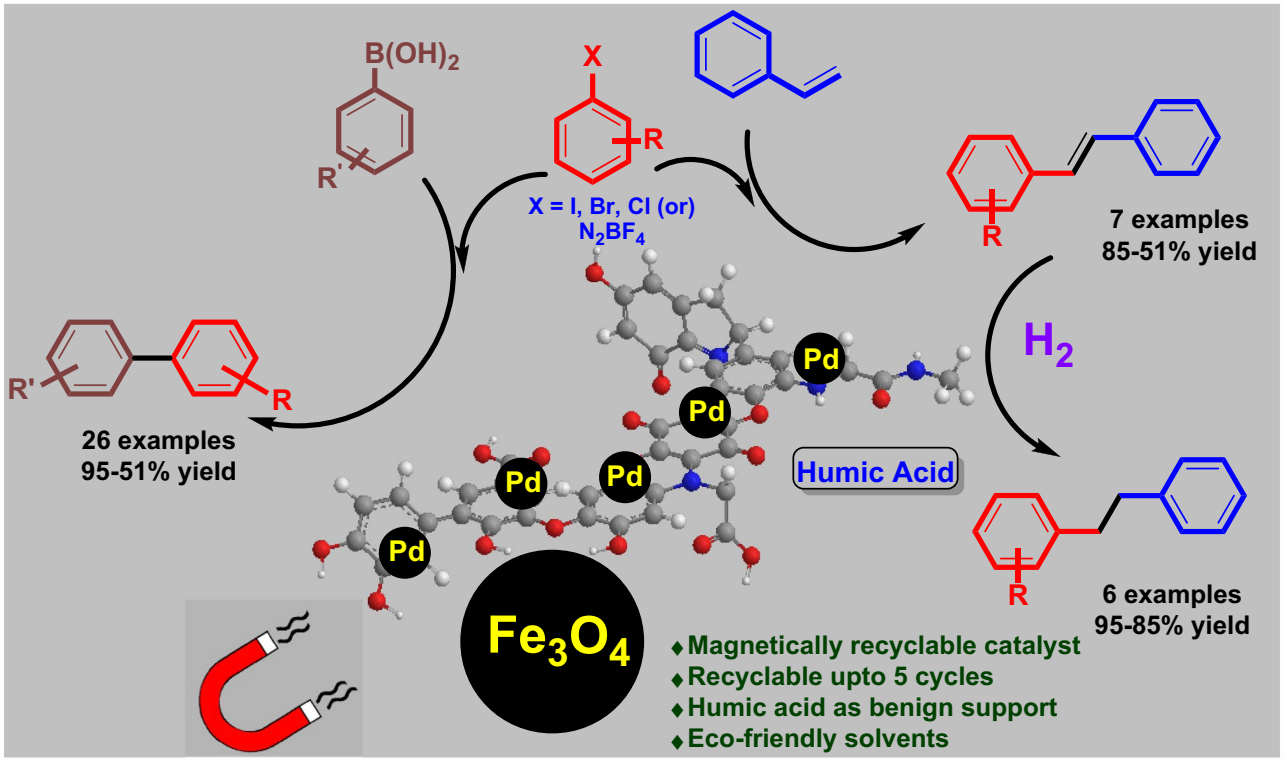

Keywords Cross-coupling · Heterogeneous · Humic acid · Magnetic nanoparticles · Palladium

1 Introduction

Transition-metal catalysts have played a major role in C–C [1] and C–hetero [2] bond forming reactions which have not only benefitted the chemical [3], pharmaceutical [4], polymer [5], and other allied industries for manufacturing a wide range of products, but also laboratory-scale organic synthesis [6–8]. Amongst all the Transition-metal catalysis, palladium based reactions i.e. Heck, Suzuki–Miyaura and other ancillary cross-coupling reactions are graded the most versatile transformations in organic synthesis owing to the efficiency and diversity [9–12]. These reactions have allowed construction of biphenyls and stilbenoids which are present in many natural products, drug molecules and biologically-active molecules (Scheme 1). Although these homogeneous catalysts demonstrate high activity and selectivity, the proclivity towards heterogeneous catalysts is rising primarily due to their ease of separation from products and reusability in successive reactions. Immobilization of active molecules or metal nanoparticles on a solid support to fabricate a heterogeneous catalytic system has gained significant importance in the past decades [10, 11]. These heterogeneous nanocatalysts are a subject of substantial research and are exemplar of "green chemistry [12–18]."

Owing to their nano-size, separation of nanocatalysts through filtration or centrifugation becomes laborious. To tackle these challenges, the development of magnetically-recoverable nanoparticles (MNPs) has proved invaluable. Among the myriad of available magnetically-recoverable nanomaterials, iron oxide has flourished tremendously chiefly because it is biocompatible, nontoxic, inexpensive and exhibits superparamagnetism [19]. However, the nanoparticles have a strong tendency to aggregate. This issue is overcome by using suitable stabilizing agents such as dopamine derivatives [20–24], silica [25–28], dendrimers [29–32], ionic liquids [33–37], graphene [38–43], natural polymers [44–48] which also have reactive sites that covalently or non-covalently bind to the catalytic units and thus can display numerous synthetic applications. Commonly, synthesis of these capped iron oxide nanoparticles requires harsh conditions, toxic precursors, inert conditions. Most essentially, they suffer from the need of sophisticated synthetic procedures for capping and stabilizing the nanoparticles [49–51]. Therefore, the development of robust catalysts which are environmentally-benign, versatile,

Scheme 1 Some natural products and drug molecules containing biphenyl and stilbene moieties

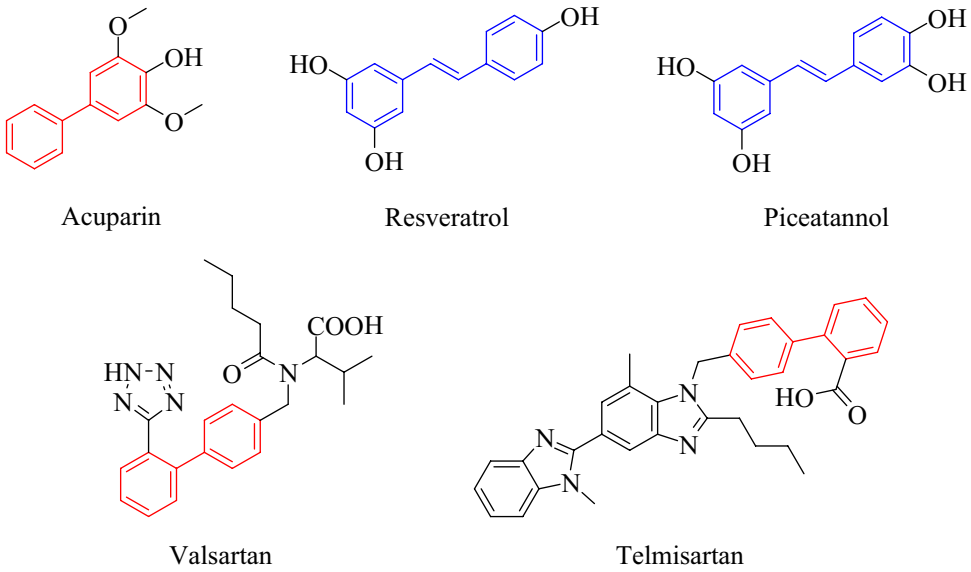

inexpensive and expediently prepared from nontoxic precursors is vital.

In light of these facts, we focused our attention towards naturally available polyphenolic substances from soil. Humic acid (HA) is one such substance found abundantly in soil along with Humic substances (HS), fulvic acid (FA) and humin [52]. Humic acid possesses multiple hydroxyl and carboxylic groups which exhibit exceptional binding capability to metal oxide nanoparticles especially iron oxides and can significantly alter their physicochemical and sorption behavior [53–55]. Besides this, due to its planar structure, humic acid shows good interaction with organic compounds especially aromatic molecules by providing large surface area. Moreover, substantial research on humic acid for sequestering heavy-metal ions and polyaromatic hydrocarbons from aquatic sources is ongoing [56–61].

Considering the sequestering capability of humic acid towards late transition metal ions, we envisaged that humic acid can act as an excellent capping agent for iron oxide nanoparticles which can capture Pd(II) ions and further be reduced to Pd(0) NPs. Therefore, extending the methodology for magnetically-recoverable nanocatalyst, we herein present an environmentally-benign humic acid coated nanoferrites [62] supported by Palladium nanoparticles for C–C cross-coupling reactions (Suzuki and Heck reaction) and reduction of olefins using molecular hydrogen to confront the challenges of recoverability, reusability, and benign support.

2 Experimental Section

2.1 Synthesis of HA@Fe_3O_4

8.5 g of $FeSO_4.7H_2O$ and 12.3 g of $FeCl_3.6H_2O$ were dissolved in 200 mL of de-ionized water in a 1000 mL beaker and heated to 90 °C. The pH of the solution was regulated by adding 30% ammonia solution (25 mL) followed by addition of sodium salt of humic acid (1 g). The solution was stirred using an overhead stirrer for 40 min and then cooled to room temperature. The particles were recovered using an external magnet followed by washing with ethanol and de-ionized water. Later, the particles were dried in a vacuum oven.

2.2 Preparation of HA@Pd/Fe_3O_4

The Fe_3O_4 coated with humic acid (HA@Fe_3O_4) MNPs were obtained from the previously reported method. In a 1000 mL beaker, 1 g of HA@Fe_3O_4 MNPs were added to 400 mL of de-ionized water and sonicated for 30 min. Meanwhile, in a 15 mL round-bottom flask, 80 mg of $PdCl_2$ and 90 mg of NaCl were dissolved in 6 mL of de-ionized water and heated to 60 °C with constant stirring till homogeneity and then, cooled to room temperature. This solution was added to the sonicated mixture of HA@Fe_3O_4 MNPs and stirred on an overhead stirrer at room temperature. Further, $NaBH_4$ solution (76 mg of $NaBH_4$ in 25 mL) was added to it portion-wise over a period of 30 min and stirred for 15 h. The resultant wet paste was recovered using an external magnet from the solution and washed with de-ionized water (50 mL × 3) and acetone (25 mL × 3). The catalyst was dried in a vacuum oven at room temperature.

2.3 General Procedure for Suzuki Cross-Coupling Between Aryl Boronic Acid and Aryl Halide

A 15 mL round bottom flask (back-filled with N_2) was loaded with HA@Pd/Fe_3O_4 (50 mg). Aryl halide (1 equiv.), aryl boronic acid (1.1 equiv.) and potassium carbonate (2.0 equiv.) were added to the flask followed by 1:1 mixture of

ethanol and water (4 mL). The resultant mixture was stirred at 50 °C for 4 h under nitrogen atmosphere. With the aid of an external magnet, the catalyst was recovered and the product was extracted using ethyl acetate (5 mL × 3). The organic layer was separated and dried over Na_2SO_4 followed by evaporation under reduced pressure and the mixture was purified using column chromatography on silica gel (Petroleum ether/Ethyl acetate).

2.4 General Procedure for Suzuki Cross-Coupling Between Aryl Diazonium Tetrafluoroborate and Aryl Boronic Acid

A 15 mL round bottom flask was loaded with HA@Pd/Fe_3O_4 (50 mg). Aryl diazonium tetrafluoroborate (1 equiv.), aryl boronic acid (1.1 equiv.) were added to the flask followed by methanol (4 mL). The resultant mixture was stirred at room temperature for 12 h in air. With the aid of an external magnet, the catalyst was recovered and the product was extracted using ethyl acetate (10 mL × 3). The organic layer was separated and dried over Na_2SO_4 followed by evaporation under reduced pressure and the mixture was purified using column chromatography on silica gel (Petroleum ether/Ethyl acetate).

2.5 General Procedure for the Heck Reaction

To a solution of aryl halide (1 equiv.), styrene (2 equiv.) and HA@Pd/Fe_3O_4 (50 mg) in DMF (4 mL), potassium carbonate (2.5 equiv.) was added. The resultant mixture was stirred under O_2 atmosphere at 140 °C for 24 h. With the aid of an external magnet, the catalyst was recovered and water (5 mL) was added to the reaction mixture. Further, the product mixture was extracted using ethyl acetate (5 mL × 3). To remove traces of DMF, the organic layer was washed with water (4 mL × 2) and then the organic layer was dried over Na_2SO_4. The solvent was evaporated under reduced pressure and the mixture was purified using column chromatography on silica gel (Petroleum ether/Ethyl acetate).

2.6 General Procedure for Olefin Reduction Using Molecular Hydrogen

In a 25 mL round bottom flask equipped with Teflon coated magnetic needle, olefin (1 equiv.) was dissolved in 4 mL of methanol. Then, H_2 was introduced in the flask followed by flushing it twice and the resulting mixture was stirred at room temperature under H_2 atmosphere for 15 h. The solvent was then evaporated under reduced pressure and water (5 mL) was added to the residue to dissolve inorganic impurities. The product was then extracted using ethyl acetate (3 × 5 mL). The organic layer was dried over sodium sulphate and the solvent was evaporated under reduced pressure. The mixture was purified using column chromatography on silica gel (Petroleum ether/Ethyl acetate).

3 Results and Discussion

Initially, humic acid capped Fe_3O_4 NPs were prepared and were used to immobilize palladium nanoparticles on them. The as synthesized material was fully characterized by Scanning Electron Microscopy (SEM), Transmission Electron Microscopy (TEM), X-Ray Diffraction (XRD), X-Ray Photoelectron Spectroscopy (XPS), Energy Dispersive Spectroscopy (EDS), Fourier Transformed Infrared Spectroscopy (FT-IR), and Inductively Coupled Plasma Atomic Emission Spectroscopy (ICP-AES) analysis. The humic acid coating is indistinguishable from SEM images (Fig. 1). For a detailed knowledge on the surface morphology, Transmission Electron Microscopy (TEM) and High-Resolution TEM (HR-TEM) of HA@Pd/Fe_3O_4 was done (Fig. 2). It was observed that humic acid is uniformly coated along with evenly distributed Pd NPs of size less than 10 nm on the catalyst. Energy Dispersive X-Ray (EDX) mapping provided the elemental composition of HA@Pd/Fe_3O_4 (Fig. 6a). The presence of palladium and carbon peaks in the spectrum confirmed the humic acid coating as well as supported palladium on the catalyst. Upon ICP-AES analysis, it was discovered that 7.98 wt% of Pd was loaded. X-ray Photoelectron Spectroscopy (XPS) was carried out for native as well as recycled HA@Pd/Fe_3O_4 to identify the chemical state of Pd supported on the catalyst. XPS analysis of the native catalyst in Pd 3d region (Fig. 7) indicates that BE of Pd $3d_{5/2}$ at 335.4 eV and $3d_{3/2}$ at 340.6 eV, which is a characteristic emissions from metallic Pd (0). The XPS data for recycled catalyst showed that the peaks did not shift, thus suggesting the unaffected chemical state of Pd after the reaction. X-ray Diffraction is a valuable technique to understand the lattice structure of a material. The XRD pattern of the obtained HA, HA@Fe_3O_4, HA@Pd/Fe_3O_4 ative and recycled) are shown (Figs. 3, 8). The peaks in the XRD pattern of HA were not as prominent as the native catalyst peaks. Native HA@Pd/Fe_3O_4 shows characteristic broad and weak (1 1 1) reflection peak centered at $2\theta = 39.5°$ indicate the presence of metallic Pd (0). This peak was visible in recycled HA@Pd/Fe_3O_4 hinting towards the presence of Pd NPs even after the 5th cycle. FT-IR of HA@Pd/Fe_3O_4 was recorded (Fig. S1, supporting information) to ascertain the functional groups in the support. The spectrum shows a strong and broad peak at 3400 cm^{-1} which is indicative of H-bonded hydroxyl groups whereas the 1720 cm^{-1} shoulder peak corresponds to the presence of ketonic or aldehydic C=O group. This was confirmed by the characteristic COO^- peaks at 1600 cm^{-1} and 1390 cm^{-1}. The band near 1600 cm^{-1} could be due to C=C aromatic vibrations and H-bonded C=O quinones. The

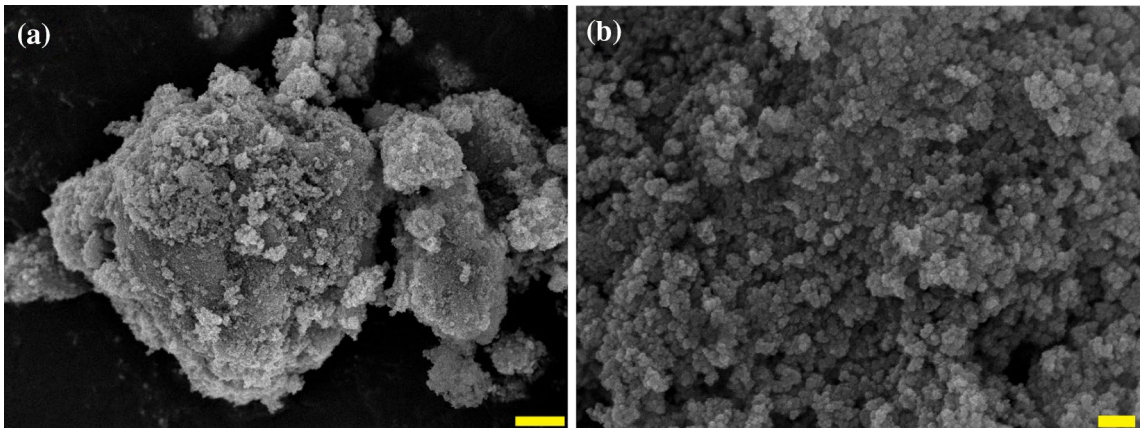

Fig. 1 SEM images of native HA@Pd/Fe_3O_4 (**a**) yellow bar shown is 1 μm length (**b**) yellow bar shown is 100 nm length

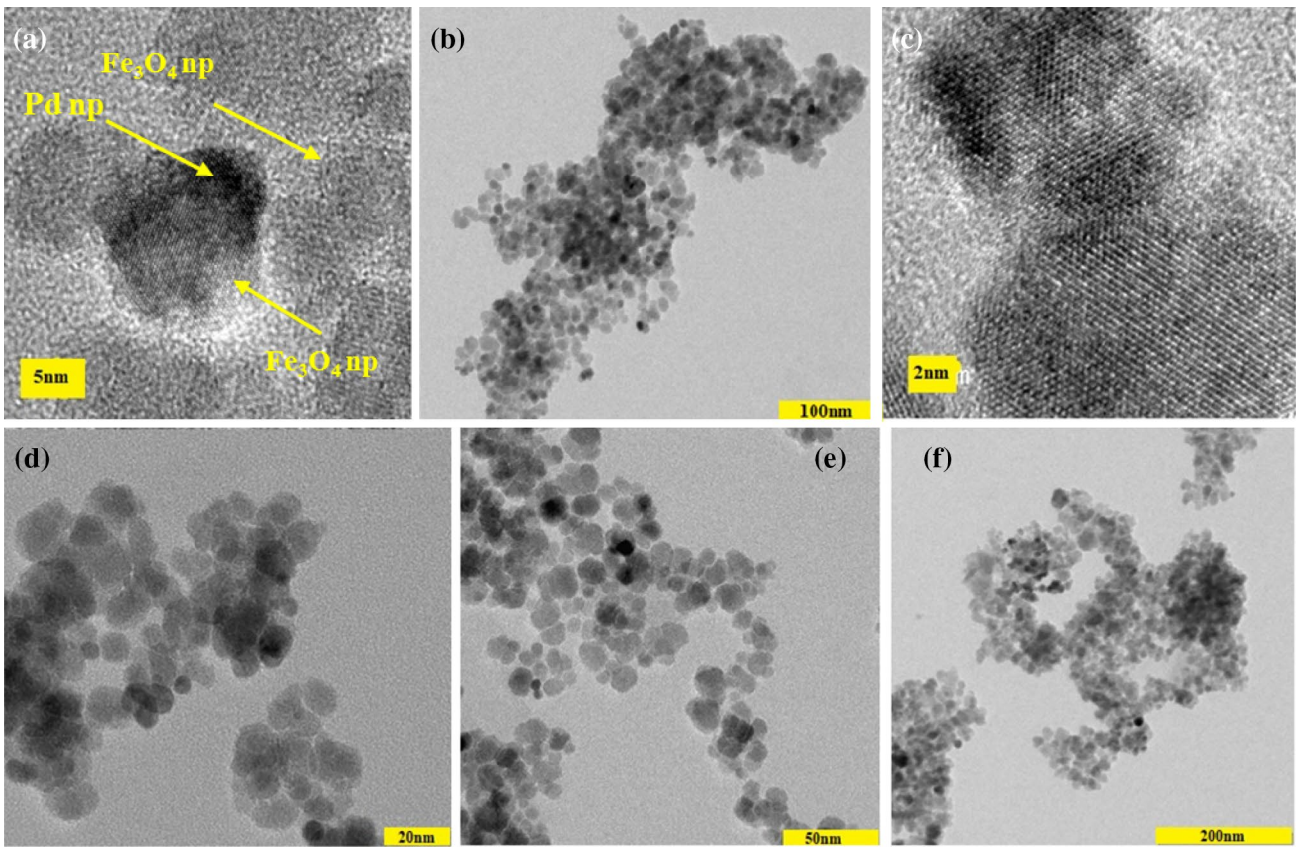

Fig. 2 HR-TEM images (**a, c**) and TEM images (**b, d**) of native HA@Pd/Fe_3O_4 and TEM images (**e, f**) of recycled HA@Pd/Fe_3O_4

strong peak at 530 cm^{-1} is characteristic of Fe–O stretching which confirms the interaction between iron oxide and humic acid [63]. All these characterization techniques conclusively authenticated the immobilization of Pd on the support. To investigate the catalytic activity of HA@Pd/Fe_3O_4, we attempted Suzuki–Miyaura cross-coupling reaction. In order to determine optimized reaction conditions, we chose the reaction between 4-iodoanisole and phenylboronic acid as a model reaction.

Several parameters such as solvent, bases and temperature of the reaction were varied to obtain the best yields. The combination of 1:1 of ethanol: water mixture with K_2CO_3 as base at 50 °C afforded the cross-coupled product in 94% yield (Table 1, entry 7). The identity of the product was

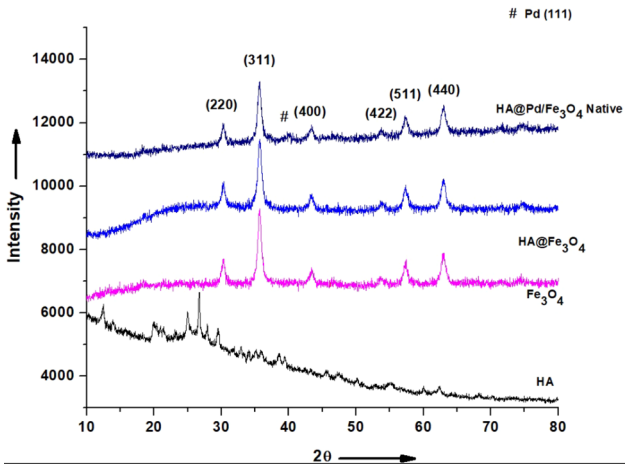

Fig. 3 XRD pattern of HA, Fe_3O_4, HA@Fe_3O_4, and HA@Pd/Fe_3O_4 (Native)

Table 1 Screening of different bases, solvents and temperatures for Suzuki cross-coupling of 4-iodoanisole and phenylboronic acid under reaction condition

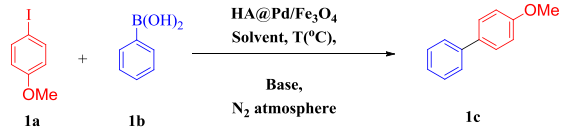

1a 1b 1c

Entry	Solvent	Base	T (°C)	Yield(%)[a]
1	Ethanol	K_2CO_3	80	93
2	Ethanol	Cs_2CO_3	80	93
3	Ethanol	Et_3N	80	90
4	Ethanol	K_2CO_3	50	92
5	Ethanol	K_2CO_3	30	85
6	Methanol	K_2CO_3	50	86
7	**Ethanol:H_2O**	**K_2CO_3**	**50**	**94**
8	Methanol:H_2O	K_2CO_3	50	88
9	Water	K_2CO_3	50	52

Reaction condition: 4-iodoanisole (0.5 mmol), phenylboronic acid (0.55 mmol), base (1 mmol), catalyst (50 mg), solvent (4 mL), N_2 atmosphere, 4 h

[a]Isolated yield

confirmed by ^{1}H and ^{13}C NMR spectroscopy. The turnover number and turnover frequency of the synthesized PdNPs are found to be 14.329 and 1.0023×10^{-3} s^{-1} respectively.

With the optimized conditions in hand, several substrates were screened for their conversion. The reaction of phenylboronic acid with aryl iodides possessing electron-withdrawing and electron-donating groups such as nitro, methoxy and cyano, afforded the products in good yields (95–89%). The aromatic heterocyclic iodides *viz*. 2-pyridyl iodide and 2-iodothiophene also gave excellent yields of 89% and 85% respectively (Tables 2, 1l and 1i).

We further extended the substrate scope by reacting substituted bromoarenes with phenylboronic acid. Different aryl bromides bearing electron-donating and electron-withdrawing groups also successfully afforded the products in 90–85% yield. The polyaromatic aryl products *viz*.,1-pyrenyl (Table 2, 1k) and 2-naphthyl (Table 2, 1f) obtained from the corresponding arylboronic acids and 4-iodoanisole were obtained in 94% and 92% yield respectively whereas the reaction of the same boronic acids with 4-bromoanisole formed products in 88% and 89% yield respectively. As anticipated the aryl halides possessing electron-donating substituents were less reactive in contrast to electron-withdrawing counterparts. For the same reason, the reaction of 4-chloroanisole with phenylboronic acid, was found to be sluggish even at higher temperature providing unsatisfactory yield of 32%. (Table 2, 1c).

It is noteworthy to mention that, the challenging reactions of aryl bromide, that too the ones with electron-donating substituents despite their low reactivity underwent conversion to afford products in good to excellent yields vouches the efficiency of the catalyst. Additionally, reactant/products bearing oxidation or hydrolysis-prone substituents such as cyano or ester groups were unaffected under these conditions and hence, no such side products formation was observed. Proficiency and mildness of the developed protocol can be advocated due to the conservation of sensitive groups and improved activation of substrates. To further examine the usefulness of the catalyst, we decided to employ it another cross-coupling reaction which is relatively unexploited with heterogeneous Pd catalysts. We carried out Suzuki–Miyaura reaction of aryldiazonium tetrafluoroborate and arylboronic acid using this catalytic system. Initially, 4-methoxyphenyldiazonium tetrafluoroborate and phenylboronic acid were chosen as model substrates for the optimization of the reaction. Parameters affecting the reaction such as solvent and temperature were varied to obtain the optimum yield of the products. The reaction when carried out in methanol as reaction solvent at 30 °C afforded the maximum yield of 88% of the biaryl product (Table 3).

To broaden the substrate scope, diverse aryldiazonium tetrafluoroborates and aylboronic acids were assessed for their conversion. Electron-withdrawing and electron-donating groups on both aryldiazonium tetrafluoroborates and arylboronic acids were well-tolerated offering yields ranging from 93 to 83% (Table 4). Only in case of 4-methoxyphenyldiazonium tetrafluoroborate and 4-nitrophenylboronic acid, the corresponding product was obtained in poor yield of 26% which shows sluggishness of the substrates to react *via* oxidative coupling mechanism (Table 4, 2e).

The Heck reaction is typically found to be difficult to accomplish using a supported palladium catalyst. Therefore,

Table 2 Suzuki cross-coupling reactions between various aryl halides with arylboronic acids with HA@Pd/Fe_3O_4 nanocatalyst

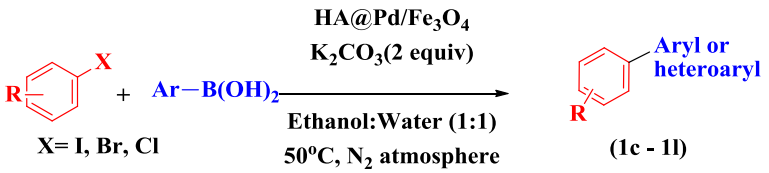

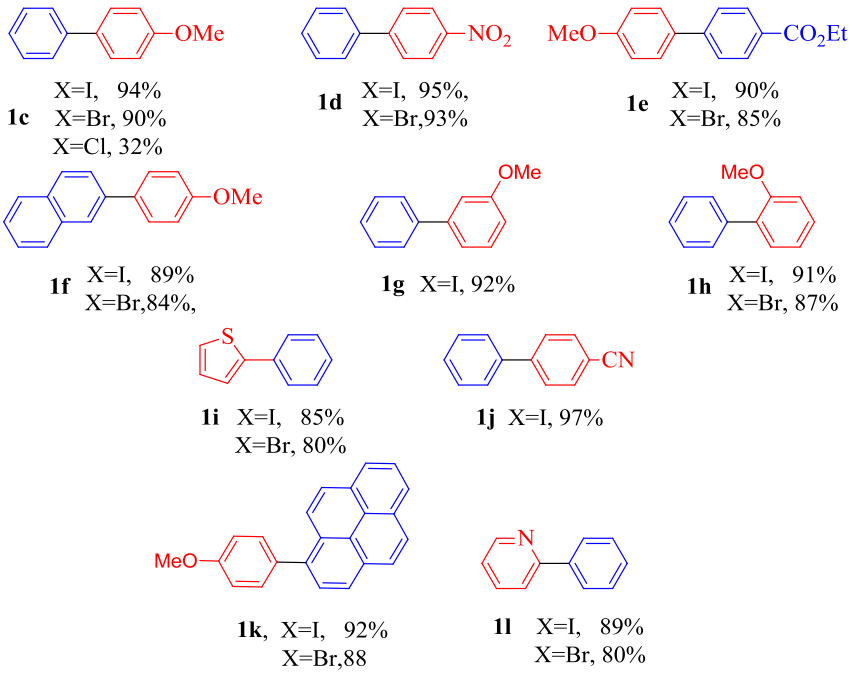

Reaction condition: arylhalide (0.5 mmol), aryl/heteroarylboronic acid (0.55 mmol), K_2CO_3 (1 mmol), HA@Pd/Fe_3O_4 (50 mg,), 4 h/6 h/ 24 h, solvent (4 mL), N_2 atmosphere

Table 3 Screening of different solvents and temperatures for Suzuki cross-coupling between aryldiazonium tetrafluoroborate and arylboronic acid under reaction conditions

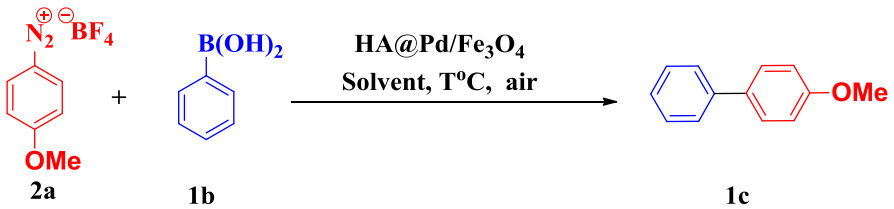

Entry	Solvent	Temperature (°C)	Yield(%)[a]
1	**Methanol**	**30**	**93**
2	Ethanol	30	60
3	THF	30	26
4	Water	30	12
5	Methanol	50	94

Reaction condition: 4-methoxyphenyldiazonium tetrafluoroborate (0.5 mmol) and phenylboronic acid (0.55 mmol), solvent (4 mL), 12 h

[a]Isolated yield

Table 4 Suzuki reaction of various arylboronic acids with aryldiazonium tetrafluoroborate using HA@Pd/Fe_3O_4 nanocatalyst[a]

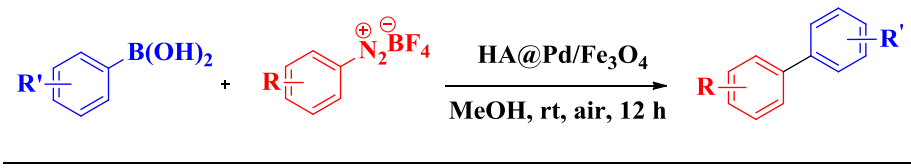

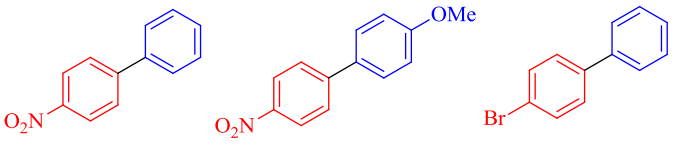

2a, 93% **2b**, 91% **2c**, 84%

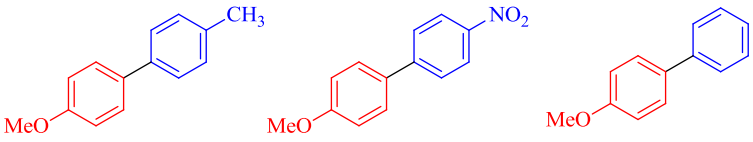

2d, 83% **2e**, 26% **2f**, 88%

Reaction condition: 4-methoxyphenyldiazonium tetrafluoroborate (0.5 mmol) and phenylboronic acid (0.55 mmol), solvent (4 mL), 12 h

[a]Isolated yield

Table 5 Screening different solvents, bases and temperature for the Heck reaction between 4-iodoanisole and styrene under reaction condition

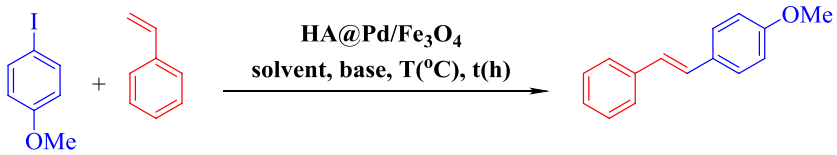

3a **3b** **3c**

Entry	Solvent	Temperature	Base	Time(h)	Yield(%)[a]
1[b]	MeCN	100	K_2CO_3	24	20
2	DMF	100	K_2CO_3	24	53
3	DMA	100	K_2CO_3	24	49
4	DMF	120	K_2CO_3	24	65
5	**DMF**	**140**	**K_2CO_3**	**24**	**77**
6	DMF	160	K_2CO_3	24	77
7	DMF	140	Et_3N	24	55
8	DMF	140	Cs_2CO_3	24	79

Reaction condition: 4-iodoanisole (0.5 mmol), styrene (1 mmol), base (1.25 mmol), solvent (3 mL), catalyst (50 mg), O_2 atmosphere

[a]Isolated yield

[b]Reaction carried out in sealed tube

Table 6 Heck reaction of different aryl halides with styrene with HA@Pd/Fe_3O_4[a]

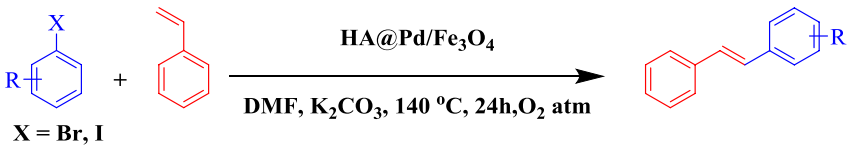

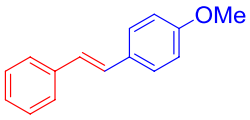

3c X = I, 77%, X=Br,51%

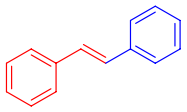

3e X=I, 80%, X=Br, 63%

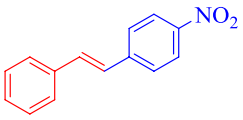

3d X=I, 85%, X=Br, 70%

Reaction condition: aryl halide (0.5 mmol), styrene (1 mmol), K_2CO_3 (1.25 mmol), DMF (3 mL), catalyst (50 mg), O_2 atmosphere, 24 h

[a]Isolated yield

Table 7 Screening of different solvent and different temperatures for reduction of olefins using molecular hydrogen

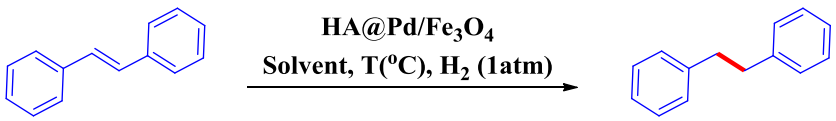

3a **3b**

Entry	Solvent	Temperature (°C)	Yield (%)[a]
1	THF	50	90
2	THF	30	88
3	**Methanol**	**30**	**95**
4	Ethanol	30	92

Reaction conditions: *(E)*-stilbene (0.5 mmol), catalyst (50 mg), solvent (4 mL), 12 h

[a]Isolated yield

we decided to investigate the robustness of this catalytic system towards the Heck reaction of aryl halides namely, aryl iodides and aryl bromides. The optimized conditions were determined by taking 4-iodoanisole and styrene as the model substrates and varying the factors affecting the reaction such as solvent, base and temperature. The optimum yield of product was obtained when DMF was taken as the reaction solvent using K_2CO_3 as base at 140 °C under O_2 atmosphere (Table 5).

The products were obtained in the range of 85–51% depending on the nature of aryl halide. As expected, a trend was observed with electron rich aryl halides which are less reactive than the electron deficient counterparts. The aryl bromides being less reactive, required longer reaction times and afforded only moderate yields of products (Table 6). However, the reaction did not proceed in the case of aryl chlorides.

Table 8 Olefin reduction using molecular hydrogen of different stilbenes with Pd/Fe_3O_4 under reaction condition[a]

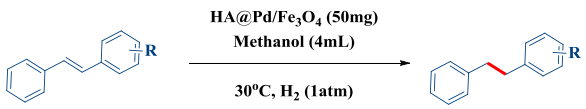

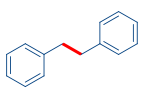

4a, 95%

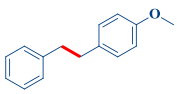

4b, 94%

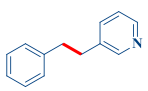

4c, 85%

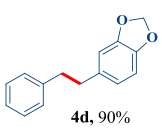

4d, 90%

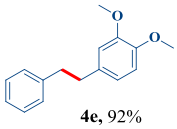

4e, 92%

Reaction conditions: olefin (0.5 mmol), catalyst (50 mg), methanol (4 mL),12 h

[a]Isolated yield

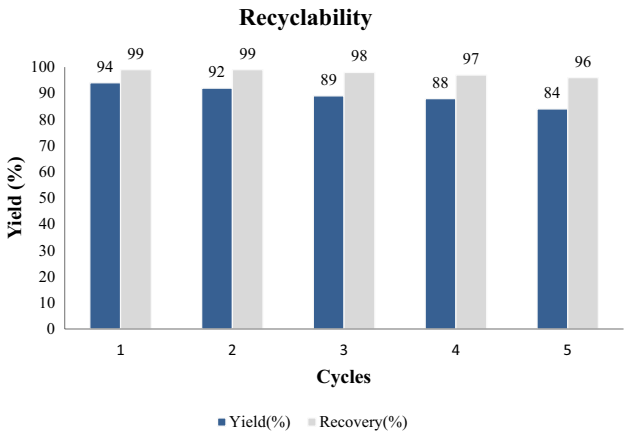

Fig. 4 Recyclability of HA@Pd/Fe_3O_4 nanocatalyst

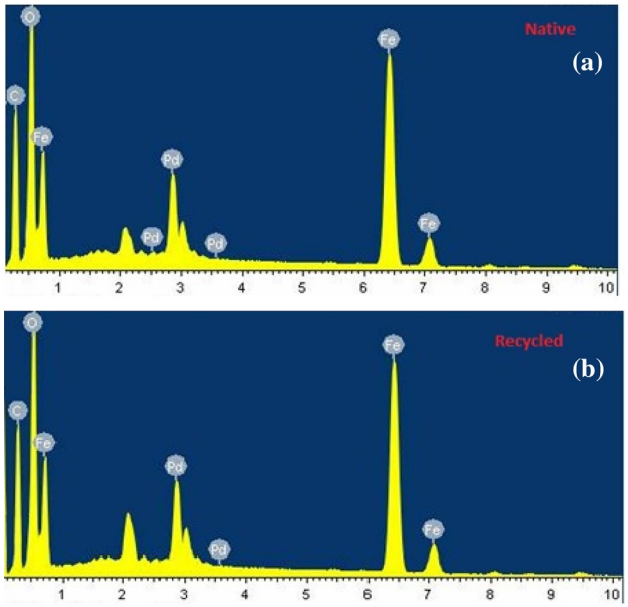

Fig. 6 EDX images of native (**a**) and recycled (**b**) catalyst

Nowadays, versatile multi-modal catalysts are highly desirable due to increasing demand in sustainable chemistry leveraging the principle "one catalyst-many jobs [47, 48]." In this context, we evaluated the versatility of HA@Pd/Fe_3O_4 catalyst for the reduction of olefins using molecular hydrogen and *trans*-stilbene as the model substrate. In order to optimize the reaction conditions, parameters such as solvent and temperature were varied. The best outcome was observed when the reaction was carried out in methanol at room temperature in 12 h (Table 7).

Applying these optimized conditions, effectiveness of this catalyst towards diverse substrates was assessed. Substituted (*E*)-stilbene derivatives were employed in order to carry out this the task and it was found that good to excellent yields of products ranging from 96 to 85% were obtained. Remarkably, the reaction proceeded smoothly without the use of a base and under mild conditions. Electron-donating as well as electron-withdrawing substituents on the stilbene were well-tolerated. When reduction of 4-nitrostilbene was carried out, an inseparable mixture of products was observed, possibly due to lack of selectivity towards C=C and nitro group leading to the formation of saturated and unsaturated amines (Table 8).

For heterogeneous catalytic systems, the level of reusability and the lifetime of a catalyst are very crucial. Therefore, we probed the recyclability of the catalyst (Fig. 4) for Suzuki cross-coupling between 4-iodoanisole and phenylboronic acid by recovering the catalyst particles and reuse them in the next cycle. The recovery of the catalyst was effortless owing to the magnetic property exhibited by iron oxide nanoparticles. Unlike the conventional laborious methods such as filtration or centrifugation, the catalyst was recovered by means of an external magnet. The nanoferrite-supported

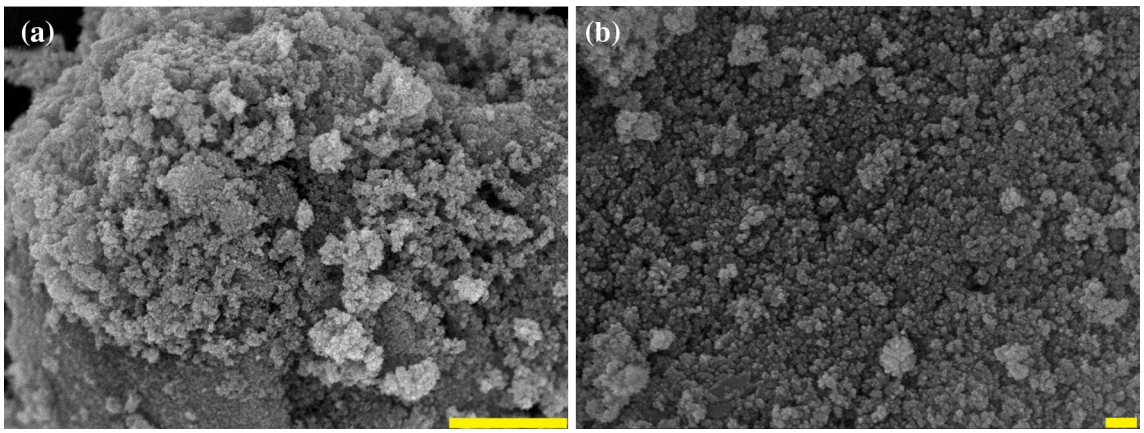

Fig. 5 SEM images of recycled HA@Pd/Fe_3O_4 (**a**) yellow bar shown is 1 μm length (**b**) yellow bar shown is 100 nm length

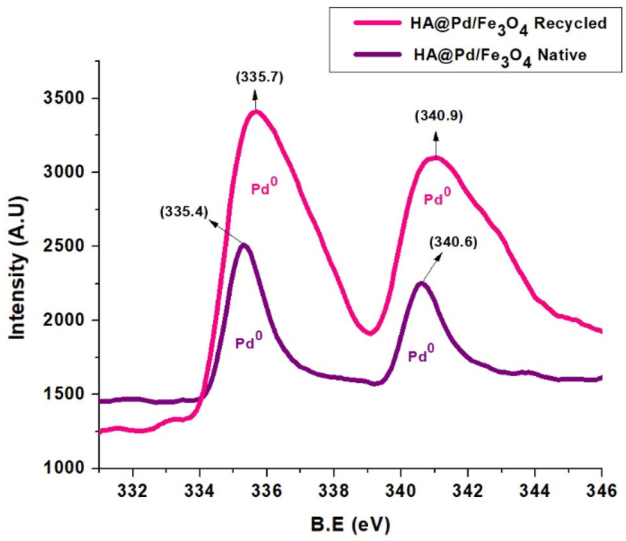

Fig. 7 XPS image of native and recycled HA@Pd/Fe_3O_4

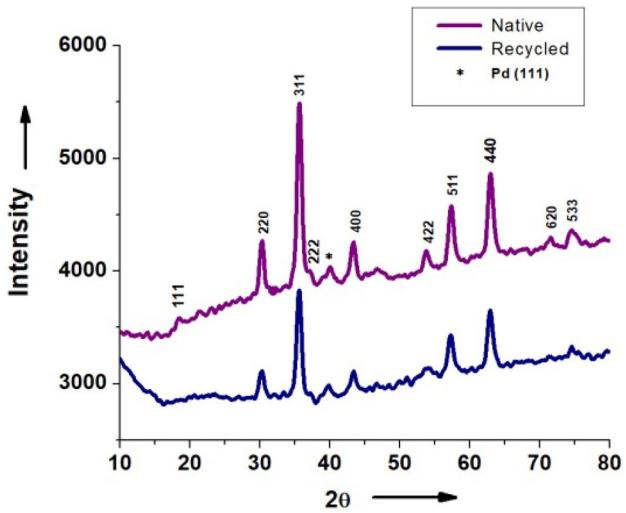

Fig. 8 XRD Pattern of native and recycled HA@Pd/Fe_3O_4

palladium catalyst showed excellent efficiency and recoverability till the fifth cycle without any loss of activity. With the completion of recyclability study, we examined the change in surface morphology the catalyst after the 5th cycle as it poses a significant difficulty in heterogeneous catalytic systems. To gain more insights of heterogeneity of the catalyst, how palladium is operating in the reaction under the optimised reaction conditions, we performed a hot filtration test. For this the cross-coupling reaction between 4-iodoanisole and phenylboronic acid was carried out for 2 h executed 62% yield of desired coupled product, later the catalyst was removed/separated magnetically. The obtained filtrate was taken in a separate reaction flask and reaction continued at 50 °C for next 24 h, shows no increase in the coupled product yield. Another hot filtration test was carried out in the same optimized condition (reaction conversion after 2 h ~ 61%) but now catalyst filtered by centrifugation (3000 rpm) to prevent the back deposition of leached if any Pd species. This showed a no further increase in yield the and hence endorse catalyst's heterogeneous property. In order to find out the amount of Palladium reamined intact on the support after the five cycles Pd was deliberately leached from the recycled HA@Pd/Fe_3O_4 catalyst and was found to be 7.93%, which shows no significant leaching occur during catalytic processes.

SEM analysis was done for the recycled catalyst which revealed that morphology of the catalyst was unchanged (Fig. 5). Moreover, EDX analysis of the recycled catalyst showed that the ratios of the peaks were very close compared to the native catalyst indicating that the elemental composition is intact (Fig. 6b). When XPS data of the catalyst after 5 cycles was examined, it revealed that Pd 3d region showed two peaks at BE 340.9 eV and at BE 335.7 eV corresponding to $3d_{3/2}$ and $3d_{5/2}$ respectively (Fig. 7). It can be inferred that since no other peaks were detected, the oxidation state of Pd is constant. The integrity of the lattice structure of the recycled catalyst was evaluated by XRD pattern. It was found that the lattice structure of the core nanoferrite and also Pd NPs is undamaged after 5 cycles (Fig. 8). The catalytic efficiency of various catalysts with respect to their product yield and other application in organic transformation, including this work is shown in Table 9 for comparison.

4 Conclusions

In conclusion, a novel and versatile Pd nanoparticles supported on humic acid stabilized nano-Fe_3O_4 (HA@Pd/Fe_3O_4) was prepared in a straightforward manner using nontoxic precursors. The catalyst displayed excellent catalytic activity towards Suzuki–Miyaura and Heck cross-coupling reactions by well-tolerating electron-donating and electron-withdrawing substituents on aryl iodides and bromides. Reduction of olefins was rendered possible at room temperature in nontoxic solvent and under base-free condition making it a highly sustainable methodology. Other advantages of this catalyst were facile recovery and extensive reusability. Moreover, humic acid played a major role in stabilizing the Fe_3O_4 as well as Pd nanoparticles.

Table 9 Catalytic performance of different catalysts in Suzuki–Miyaura cross-coupling and other reactios

Entry	Catalyst	Conditions	X	Time (h)	Yield (%)	Reactions	References
1	Pd-NPs@Oak Gum (0.3)	K_2CO_3, H_2O, 80 °C	I,Br,Cl	1.0, 2.0, 18.0	96,92,70	Suzuki–Miyaura cross-coupling and reduction of Nitroarenes	[14]
2	Fe_3O_4@TA/Pd (0.21)	K_2CO_3 EtOH/H_2O,25 °C	I,Br,Cl	1.5, 3.0, 24.0	98, 96, 45	Suzuki–Miyaura cross-coupling and reduction of Nitrophenol	[18]
3	Pd/Fe_3O_4@PDA (0.46)	K_2CO_3 EtOH/H_2O,80 °C	I,Br	6.0, 8.0	98, 88	Suzuki–Miyaura cross-coupling	[20]
4	Fe_3O_4@SiO_2/isoniazide/Pd (0.2)	K_2CO_3, H_2O/EtOH, r.t	I, Br	0.5, 1.5	96, 96	Suzuki–Miyaura cross-coupling and reduction of Nitrophenol	[28]
5	Fe_3O_4/IL/Pd (0.20)	EtOH/H_2O, K_2CO_3, rt	I,Br,Cl	0.25, 1.0, 18.0	96, 95, 75	Suzuki–Miyaura cross-coupling	[39]
6	Pd@PS-Met (0.1)	K_2CO_3, H_2O, 80 °C	I,Br	2.0, 4.0	96, 96	Suzuki–Miyaura cross-coupling	[52]
7	Pd-isatin Schiff base-γ-Fe_2O_3 (0.5, 1.5)	Et_3N, Solvent-free,100 °C	I, Br	0.5, 0.7	95, 90	Mizoroki–Heck coupling	[64]
8	HA@Pd/Fe3O4 (0.65)	EtOH/H2O, K_2CO_3, 50 °C	I,Br,Cl	4, 6, 24	94,90,32		This work

Acknowledgements AVD is grateful to University Grants Commision (UGC) for the research fellowship. AVK is grateful to DST, Govt. of India, for research funding, DST-SERB (YSS/2015/002064) and the Department of Pharmaceutical Science and Technology, ICT, for NMR analysis. We are also thankful to Sophisticated Analytical Instruments Facility (SAIF) at the Indian Institute of Technology, Mumbai (IITB) for providing the characterization data for the analysis of the catalyst.

References

1. Molnár (2011) Á Chem Rev 111:2251
2. Hartwig JF Nature (2008) *455*: 314
3. Blaser HU, Catal Today (2000) *60*:161
4. Busacca CA, Fandrick DR, Song JJ, Senanayake CH (2011) Adv Synt Catal 353:1825
5. Vandenberg EJ (1992) Catalysis in polymer synthesis. American Chemical Society, Washington, DC, pp 2–23
6. Feng J, Holmes M, Krische MJ (2017) Chem Rev 117:12564
7. Trost BM (1995) Angew Chem Int Ed 34:259
8. Fumagalli G, Stanton S, Bower J (2017) F, Chem Rev 117:9404
9. Chen X, Engle KM, Wang DH, Yu JQ (2009) Ang Chem Int Ed 48:5094
10. Polshettiwar V, Luque R, Fihri A, Zhu H, Bouhrara M, Basset J-M (2011) Chem Rev 111:3036
11. Wang D, Astruc D (2017) Chem Soc Rev 46:816
12. Zhang S, Nguyen L, Zhu Y, Zhan S, Tsung CK, Tao F (2013) Acc Chem Res 46:1731
13. Fihri A, Bouhrara M, Nekoueishahraki B, Basset JM, Polshettiwar V (2011) Chem Soc Rev 40:5181
14. Veisi H, Nasrabadi NH, Mohammadi P (2016) Appl Organomet Chem 30:890
15. Lebaschi S, Hekmati M, Veisi HJ (2017) Colloid Interface Sci 485:223
16. Veisi H, Faraji AR, Hemmati S, Gil A (2015) Appl Organomet Chem 29:517
17. Das SK, Parandhaman T, Pentela N et al (2014) J Phys Chem C 118:24623
18. Veisi H, Pirhayati M, Kakanejadifard A et al ChemistrySelect (2018) 3:1820
19. Karimi B, Mansouri F, Mirzaei HM, ChemCatChem (2015) 7:1736
20. Dubey AV, Kumar AV, Adv RSC (2016) 6:46864
21. Farzad E, Veisi H (2018) J Ind Eng Chem 60:114
22. Baig RBN, Varma RS (2012) Chem Commun 48:2582
23. Nasir Baig RB, Leazer J, Varma RS, Clean Technol Environ Policy (2015), 17:2073
24. Dam B, Patil RA, Ma YR, Pal AK (2017) New J Chem 41:6553
25. Jha A, Patil CR, Garade AC, Rode CV (2013) Ind Eng Chem Res 52:9803
26. Yi DK, Lee SS, Ying JY (2006) Chem Mater 18:2459
27. Sharma RK, Yadav M, Gawande MB (2016) In: Eds.: Sharma VK, Doong R, Kim H, Varma RS, Dionysiou DD ACS Symp Ser. American Chemical Society, Washington, DC, pp 1–38
28. Heidari F, Hekmati M, Veisi H (2017) J Colloid Interface Sci 501:175
29. Rehm TH, Bogdan A, Hofmann C, Löb P, Shifrina ZB, Morgan DG, Bronstein LM (2015) ACS Appl Mater Interfaces 7:27254
30. Deraedt C, Wang D, Salmon L, Etienne L, Labrugère C, Ruiz J, Astruc D, ChemCatChem (2015) 7:303
31. Asadi B, Mohammadpoor-Baltork I, Tangestaninejad S, Moghadam M, Mirkhani V, Landarani-Isfahani A (2016) New J Chem 40:6171
32. Paez JI, Froimowicz P, Landfester K, Brunetti V, Strumia M (2014) J Polym Sci Part A 52:3185
33. Safaei S, Mohammadpoor-Baltork I, Khosropour AR, Moghadam M, Tangestaninejad S, Mirkhani V, Kia R (2012) RSC Adv 2:5610
34. Zheng X, Luo S, Zhang L, Cheng JP (2009) Green Chem 11:455
35. Otokesh S, Kolvari E, Amoozadeh A, Koukabi N, RSC Adv (2015) 5:53749
36. Zhang Q, Su H, Luo J, Wei Y (2012) Green Chem 14:201
37. Mandal P, Chattopadhyay AP, Dalton Trans (2015), 44:11444
38. Jamatia R, Gupta A, Pal AK (2017) ACS Sustain Chem Eng 5:7604
39. Veisi H, Pirhayati M, Kakanejadifard A (2017) Tetrahedron Lett 58:4269

40. Zhang M, Liu YH, Shang ZR, Hu HC, Zhang ZH, Catal Commun (2017) 88:39
41. Patil MR, Kapdi AR, Vijay Kumar A (2018) ACS Sustain Chem Eng 6:3264
42. Ko S, Jang J (2006) Angew Chem Int Ed 45:7564
43. Jawale DV, Gravel E, Boudet C et al (2015) Catal Sci Technol 5:2388
44. Reddy LH, Arias JL, Nicolas J, Couvreur P (2012) Chem Rev 112:5818
45. Korneva G, Ye H, Gogotsi Y, Halverson D, Friedman G, Bradley JC, Kornev KG (2005) Nano Lett 5:879
46. Veisi H, Mirzaee N (2018) Appl Organomet Chem 32:e4067
47. Yang S, Zong P, Ren X, Wang Q, Wang X (2012) ACS Appl Mater Interfaces 4:6891
48. Veisi H, Mohammadi Biabri P, Falahi H (2017) Tetrahedron Lett 58:3482
49. Wang D, Liu W, Bian F, Yu W (2015) New J Chem 39:2052
50. Parandhaman T, Pentela N, Ramalingam B et al (2017) ACS Sustain Chem Eng 5:489
51. Veisi H, Najafi S, Hemmati S (2018) Int J Biol Macromol 113:186
52. Veisi H, Mirshokraie SA, Ahmadian H (2018) Int J Biol Macromol 108:419
53. Kharisov BI, Kharissova OV, Dias HVR (2014) Nanomaterials for environmental protection. Wiley, Hoboken, pp 483–501
54. Hu JD, Zevi Y, Kou XM, Xiao J, Wang XJ, Jin Y (2010) Sci Total Environ 408:3477
55. Ni L, Su L, Li S, Wang P, Li D, Ye X, Li Y, Li Y, Li Y, Wang C (2017) Environ Toxicol Chem 36:1856
56. Lippold H, Gottschalch U, Kupsch H (2008) Chemosphere 70:1979
57. Liu S, Zhu Y, Liu L, He Z, Giesy JP, Bai Y, Sun F, Wu F (2018) Environ Pollut 234:726
58. Tan L, Wang X, Tan X, Mei H, Chen C, Hayat T, Alsaedi A, Wen T, Lu S, Wang X (2017) Chem Geol 464:91
59. Tang Z, Zhao X, Zhao T, Wang H, Wang P, Wu F, Giesy JP (2016) Environ Sci Technol 50:8640
60. Liu J, Zhao Z, Jiang G (2008) Environ Sci Technol 42:6949
61. Stevenson FJ, Goh KM (1971) Geochim Cosmochim Acta 35:471
62. García-Suárez EJ, Balu AM, Tristany M, García AB, Philippot K, Luque R (2012) Green Chem 14:1434
63. García CS, Uberman PM, Martín SE, Beilstein (2017) J Org Chem 13:1717
64. Sobhani S, Zarifi F, Chinese J, Catal (2015), 36:555